Sigma-Aldrich®
Lab Materials & Supplies

ISOTEC® Stable Isotopes

Products for MRI/MRS and PET Imaging

- Hyperpolarization
- MRI/MRS
- Noble Gases
- PET Imaging

MilliporeSigma

Dynamic Nuclear Polarization

Dr. Matthew E. Merritt, Assistant Professor,
Advanced Imaging Research Center,
Southwestern Medical Center at Dallas

Dynamic Nuclear Polarization (DNP) is a phenomenon by which high spin polarization, typically derived from a bath of free radical electrons, is transferred to a nuclear spin bath, enhancing the difference between the nuclear energy levels and thereby producing dramatically enhanced NMR signals for detection. The phenomenon was first predicted by Overhauser,[1] but was not observed experimentally until the work of Slichter in metals in 1953.[2] It was soon understood that the same technique could be used to develop high polarizations of ^{1}H, ^{2}H, and ^{13}C in non-conducting solids. This advance became foundational for production of solid targets for high energy physics research.[3–5] High nuclear polarizations in the targets simplified the results of neutron scattering experiments. Subsequently, the DNP method migrated to chemistry, being used to study a variety of structural questions in the solid state.[6, 7] Robert Griffin of MIT has pioneered the use of DNP for signal enhancement in solid state NMR distance measurements for structural biology.[8] In his method, a water soluble free radical is doped into a matrix containing H_2O/glycerol and the solute molecule/protein to be studied. This method has recently been used to study the K intermediate of bacteriorhodopsin in intact purple membrane.[9] While DNP is also possible in the liquid state, it is much less efficient due to the diminishment of the intermolecular dipolar couplings by fast molecular tumbling.[10]

The production of hyperpolarized molecular imaging agents has sparked great enthusiasm in the MRI community due to its potential application as a clinically viable method for assessing *in vivo* metabolism. Golman and co-workers demonstrated that a hyperpolarized solid may be rapidly melted with a bolus of boiling water and shuttled out of the DNP system using high pressure helium gas.[11] The hyperpolarized solute molecule can be used as an imaging agent[12–14]. The most popular molecule to date for hyperpolarization studies has been [1-^{13}C]pyruvate, though other common metabolites have also been used successfully. This technique now stands as one of the most promising new methods for measuring *in vivo* metabolism.

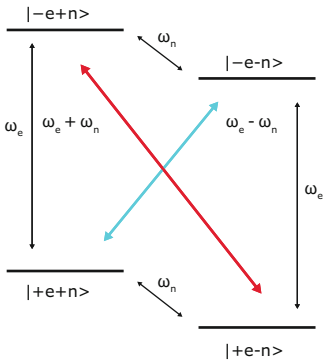

Figure 1. Energy level diagram for a coupled electron-nuclear spin system. The normally forbidden transitions (colored arrows) can be excited by microwave irradiation, resulting in dramatically increased nuclear polarizations.

Dynamic Nuclear Polarization

The DNP phenomenon was first recognized as theoretically possible as an outflow of basic research into the nature of cross relaxation in NMR. Figure 1 shows the energy level diagram for a single electron coupled to a nuclear spin in a strong magnetic field. The gyromagnetic ratio for an electron spin is ~2400 times greater than that of a ^{13}C nucleus. Therefore the single quantum transitions associated with the electrons are in the gigahertz regime (94 GHz at 3.35T) while the carbon Larmor frequency is ~35 MHz. Normally, zero (Figure 1 red arrow) or double quantum transitions (Figure 1 green arrow) are strictly forbidden. However, the hyperfine coupling between the spins is of sufficient magnitude that the 4 energy levels are not pure states, and consequently these transitions become partially allowed. Under microwave irradiation at the electron resonance frequency ± the nuclear frequency these transitions are stimulated and the nuclear polarization is enhanced in a positive or negative manner depending on the transition that is irradiated (Figure 2). This is known in the literature as the solid effect. This mechanism is active when the electron resonance has a linewidth of the same order or less than the nuclear Larmor frequency. This is commonly the case when the trityl radical is used for polarizing protons. However, at 3.35T, the FWHM of the electron resonance is ~44 MHz.[15] Therefore, when using trityl and ^{13}C, the thermal mixing mechanism is likely the main source of polarization. Thermal mixing is another DNP mechanism that is active when the electron resonance is wider than the nuclear Larmor frequency, as is common when nitroxide radicals such as TEMPO are used or when lower γ nuclei are the targets. An excellent description of the differences between the two mechanisms is outlined in the paper by Comment, et. al.[16] In a somewhat simplified picture, thermal mixing is a three spin effect as opposed to two in the solid effect. It also depends upon strong dipolar couplings between electron spins, in effect, the presence of an electron spin bath that can be described with a single temperature. Irradiation of the bath at a certain frequency causes other coupled electron spins to flip. Since the spins at other resonance frequencies have slightly different energies, the difference can be made up with a coupled nuclear spin. Since a difference in frequencies is still necessary like in the solid effect, thermal mixing again produces characteristic positive and negative enhancements, though the maxima are separated by a number closer to the Larmor frequency of the nucleus (Figure 2). Traditionally, it has been understood that the solid effect required more power than thermal mixing since forbidden transitions are pumped. In thermal mixing, no forbidden transitions are present and therefore it might be expected to be a more efficient mechanism. This likely explains the extremely high polarizations achievable when using trityl and ^{13}C. New bi-radicals seek to increase the available polarization by tethering the free electrons together, resulting in stronger electron dipolar couplings and enhancing thermal mixing for protons.[17]

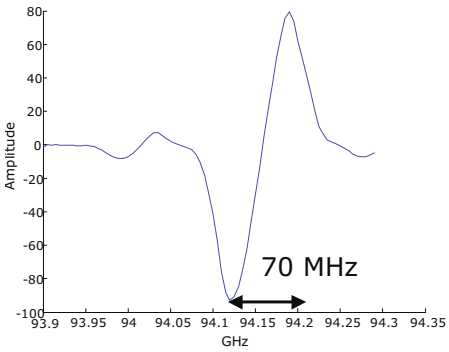

Figure 2. DNP enhancement curve as a function of frequency for [1-^{13}C]pyruvate mixed with the trityl radical. Each data point was collected after irradiation for 300 seconds, which is not long enough to reach the equilibrium polarization. The 70 MHz splitting observed would lead one to believe that the solid effect is active, but longer irradiation times show a splitting between the maxima of ~63 MHz, indicating thermal mixing as the source of enhancement.

Fast Dissolution DNP

The DNP method developed by Golman and co-workers has several essential elements that allow the spectacular signal enhancements seen to date.[11] First, the experiment is carried out at 1.2 to 1.4 K. At room temperature, the enhancement from DNP goes as the ratio of the gyromagnetic ratios of the dipolar coupled spins. At these very low temperatures, the Boltzmann distribution begins to display exponential behavior; at 1.4 K the electrons are ~92% polarized as opposed to less than 1% for ^{1}H and ^{13}C. Consequently, DNP at low temperatures can produce nuclear polarizations in the percent range as well, which is far greater than the enhancement available at room temperature. The second key insight was the realization that the sample could be melted on a time-scale fast enough that large polarizations were left over after the dissolution. The developed polarization decays with the normal T_1 of the nucleus. If the melting is slow, sufficient sensitivity is not retained in the experiment. Typically, melting of a 40 to 200 µl DNP sample is accomplished with 3 mL–6 mL of water at ~190°C and 10 bar of pressure supplied by a compressed helium tank. Due to the constraints imposed by the decay of the magnetization, protonated carbons are typically more difficult to use for DNP. C-1 labeled pyruvate has been a metabolite of choice since the C-3 protons are distal from the observed carbon. Hence, the primary source of relaxation arises from the chemical shift anisotropy. The T_1 of the C-1 carbon of pyruvate is close to 1 minute at 1.5 Tesla and ~40 seconds at 14.1 T.

Metabolism using Hyperpolarization Technique

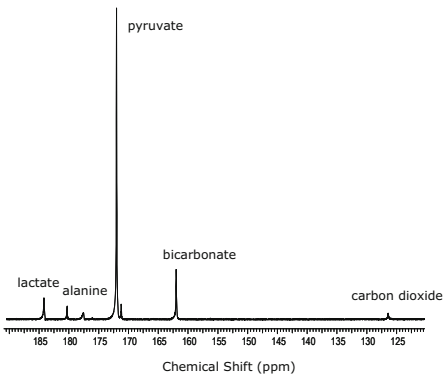

Figure 3. Carbon-13 NMR spectrum of a perfused mouse heart following injection of 2 mM hyperpolarized [1-^{13}C]pyruvate. The spectrum is a sum of 70 scans. All metabolites generated from the pyruvate are also ^{13}C labeled.

The central feature that makes imaging or spectroscopy using hyperpolarized ^{13}C labeled compounds so appealing is the incredible gains in signal to noise that can be achieved, allowing observation of biochemical reactions *in vivo* and *in vitro* that previously could not be monitored with any technique (Figure 3). The most common example, hyperpolarized [1–^{13}C]pyruvate illustrates the high information content of MR combined with hyperpolarization in powerful fashion. Figure 4 shows the information available by three different methods for assessing metabolism. Assume that three different samples have been prepared, a ^{11}C labeled pyruvate, [3-^{13}C]pyruvate, and hyperpolarized [1-^{13}C]pyruvate, for injection into a commonly used model of metabolism, the perfused rat heart. Observation of the ^{11}C compound by positron emission tomography (PET) will reveal only the uptake of the pyruvate, producing the familiar dose-response curve (Figure 4, A). Observation of the delivery of the [3-^{13}C]pyruvate by NMR would allow not only the uptake of the pyruvate to be monitored, but also its subsequent metabolism to lactate and alanine. It has been shown that detection of the label using indirect methods such as heteronuclear multiple quantum coherence (HMQC) can allow time points to be taken approximately every 10–20 seconds (Figure 4, B).[18] The bottom panel shows the data that would be obtained following injection of the hyperpolarized substrate (Figure 4, C). Due to the increase in signal to noise, time points can be taken every second, or even faster. Also, since direct detection of the ^{13}C label is possible, flux into CO_2 and bicarbonate is detectable as well. In this lab, the signal to noise gain for the hyperpolarization experiment versus the HMQC method is approximately 50 times, with the bonus of much higher resolution as a function of time following the injection. The power of this technique has already been taken advantage of to study a variety of questions with physiological and pathological significance. Hyperpolarized $H^{13}CO_3^-$ has been used as a means of assessing pH by monitoring the equilibrium between CO_2 and bicarbonate.[19] This method of pH measurement has the unique advantage of injecting a completely benign compound as the sensor. Hyperpolarized [1-^{13}C]pyruvate has been used to measure substrate preference in a perfused heart model, demonstrating the ability to assess flux through a single enzyme catalyzed reaction.[20] Workers at Cambridge University and UCSF have already shown that the kinetics of dispersal of hyperpolarized pyruvate is sensitive to cancer *in vivo*.[21–23] Cardiac dysfunction following myocardial infarction could also potentially be detected with this method.[24,25]

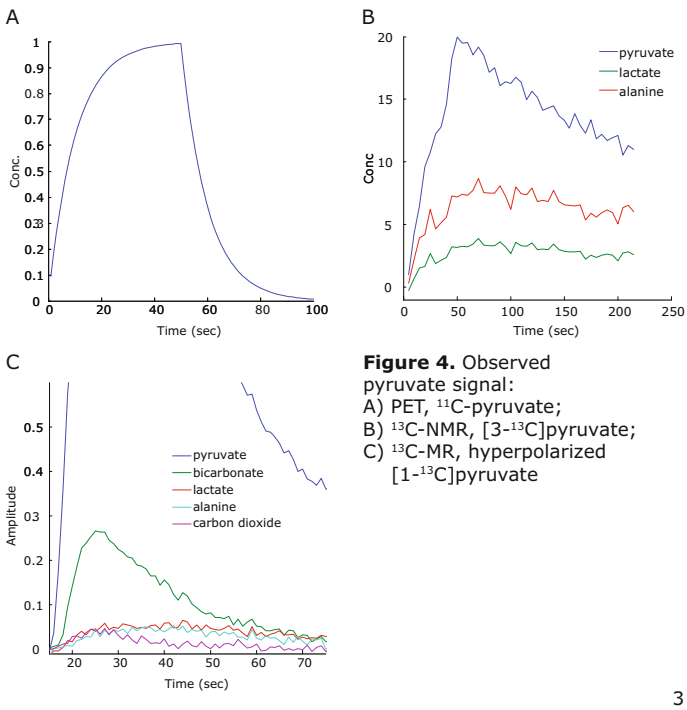

Figure 4. Observed pyruvate signal:
A) PET, ^{11}C-pyruvate;
B) ^{13}C-NMR, [3-^{13}C]pyruvate;
C) ^{13}C-MR, hyperpolarized [1-^{13}C]pyruvate

Conclusion

In summary, hyperpolarization of ^{13}C compounds is an extremely promising new avenue for molecular imaging and metabolism studies. Applications to cancer and cardiac metabolism are currently under development. Clinically relevant measures of metabolism with this technique should become available during the next decade.

References

1. Overhauser, *A. W. Polarization of Nuclei in Metals. Physical Review* **1953***, 92(2)*, 411-415.
2. Carver, T. R.; Slichter, C. P. *Polarization of Nuclear Spins in Metals. Physical Review* **1953**, *92(1)*, 212–213.
3. Abragam, A.; Goldman, M. *Nuclear Magnetism: Order and Disorder. Oxford: Oxford University Press;* **1982**, 625 p.
4. de Boer, W. *Dynamic orientation of nuclei at low temperatures. Journal of Low Temperature Physics* **1976**, *22(1)*, 185–212.
5. de Boer, W.; Borghini, M.; Morimoto, K.; Niinikoski, T. O.; Udo, F. *Dynamic Polarization of Protons, Deuterons, and Carbon-13 Nuclei: Thermal Contact Between Nuclear Spins and an Electron Spin-Spin Interaction Resevoir. Journal of Low Temperature Physics* **1974***; 15(3–4)*, 249–267.
6. Afeworki, M.; McKay, R. A.; Schaefer, J. *Selective observation of the interface of heterogeneous polycarbonate/polystyrene blends by dynamic nuclear polarization carbon-13 NMR spectroscopy. Macromolecules* **1992**, *25(16)*, 4084–4091.
7. Wind, R. A.; Duijvestijn, M. J.; Van der Lugt, C.; Manenschijn, A.; Vriend, J. A*pplications of dynamic nuclear polarization in carbon-13 NMR in solids. Progress in Nuclear Magnetic Resonance Spectroscopy* **1985***, 17(1)*, 33–67.
8. Gerfen, G. J.; Becerra, L. R.; Hall, D. A.; Griffin, R. G.; Temkin, R. J.; Singel, D. J. *High frequency (140 GHz) dynamic nuclear polarization: Polarization transfer to a solute in frozen aqueous solution. Journal of Chemical Physics* **1995***, 102(24)*, 9494.
9. Mak-Jurkauskas, M. L.; Bajaj, V. S.; Hornstein, M. K.; Belenky, M.; Griffin, R. G.; Herzfeld, J. *Energy transformations early in the bacteriorhodopsin photocycle revealed by DNP-enhanced solid-state NMR. Proceedings of the National Academy of Sciences* **2008***;105(3)*, 883–888.
10. Loening, N. M.; Rosay, M.; Weis, V.; Griffin, R. G. Solution-State *Dynamic Nuclear Polarization at High Magnetic Field. Journal of the American Chemical Society* **2002***, 124(30)*, 8808–8809.
11. Ardenkjaer-Larsen, J. H.; Fridlund, B.; Gram, A.; Hansson, G.; Hansson, L.; Lerche, M. H.; Servin, R.; Thaning, M.; Golman, K.; *Increase in signal-to-noise ratio of > 10,000 times in liquid-state NMR. Proceedings of the National Academy of Sciences of the United States of America* **2003***, 100(18)*, 10158–10163.
12. Golman, K., In't Zandt, R.; Lerche, M. H.; Pehrson, R.; Ardenkjaer-Larsen, J. H.; *Metabolic imaging by hyperpolarized ^{13}C magnetic resonance imaging for in vivo tumor diagnosis. Cancer Research* **2006***, 66(22)*, 10855–10860.
13. Golman, K.; in't Zandt, R.; Thaning, M. *Real Time Metabolic Imaging. Proceedings of the National Academy of Sciences of the United States of America* **2006***, 103(30)*, 11270–11275.
14. Golman, K.; Petersson, J. S. *Metabolic imaging and other applications of hyperpolarized ^{13}C. Academic Radiology* **2006**;13:932–942.
15. Wolber, J.; Ellner, F.; Fridlund, B.; Gram, A.; Jóhannesson, H.; Hansson, G.; Hansson, L. H.; Lerche, M. H.; Månsson, S.; Servin, R.; Thaning, M.; Golman, K.; Ardenkjær-Larsen, J. H. *Nuclear Instruments and Methods in Physics Research Section A: Accelerators, Spectrometers, Detectors and Associated Equipment* **2004**, *526*, 173–181.
16. Comment, A.; van den Brandt, B.; Uffmann, F.; Kurdzesau, F.; Jannin, S.; Konter, A.; Hautle, P.; Wenckebach, W. T.; Gruetter, R.; vander Klink, J. J. *Design and performance of a DNP prepolarizer coupled to a rodent MRI scanner. Concepts in Magnetic Resonance Part B: Magnetic Resonance Engineering* **2007***, 31B(4)*, 255–269.
17. Hu, K. N.; Yu, H. H.; Swager, T. M.; Griffin, R. G. *Dynamic Nuclear Polarization with Biradicals. J Am Chem Soc.* **2004***, 126(35)*, 10844–10845.
18. Burgess SC, Babcock EE, Jeffrey FMH, Sherry AD, Malloy CR. *NMR indirect detection of glutamate to measure citric acid cycle flux in the isolated perfused mouse heart. FEBS Letters* 2001*;505(1)*:163-167.
19. Gallagher FA, Kettunen MI, Day SE, Hu D-E, Ardenkjaer-Larsen JH, Zandt Rit, Jensen PR, Karlsson M, Golman K, Lerche MH, Brindle KM. *Magnetic resonance imaging of pH in vivo using hyperpolarized ^{13}C-labelled bicarbonate. Nature 2008; 453 (7197)*:940-943.
20. Merritt, M. E.; Harrison C.; Storey, C. J.; Jeffrey, F. M. H.; Sherry, A. D.; Malloy, C. R. *Hyperpolarized ^{13}C allows a direct measure of flux through a single enzyme-catalyzed step by NMR. Proceedings of the National Academy of Sciences of the United States of America* **2007***, 104(50),* 19773–19777.
21. Albers, M. J.; Bok, R.; Chen, A. P.; Cunningham, C. H.; Zierhut M. L.; Zhang, V. Y.; Kohler, S. J.; Tropp, J.; Hurd, R. E.; Yen, Y-F; Nelson, S. J.; Vigneron, D. B.; Kurhanewicz, J. *Hyperpolarized ^{13}C Lactate, Pyruvate, and Alanine: Noninvasive Biomarkers for Prostate Cancer Detection and Grading. Cancer Res* **2008***, 68(20)*, 8607–8615.
22. Chen, A. P.; Albers, M. J.; Cunningham, C. H.; Kohler, S. J.; Yen, Y-F.; Hurd, R. E.; Tropp, J.; Bok, R.; Pauly, J. M.; Nelson, S. J.; Kurhanewicz, J.; Vigneron, D. B*. Hyperpolarized C-13 spectroscopic imaging of the TRAMP mouse at 3T - Initial experience. Magnetic Resonance in Medicine* **2007***, 58(6),* 1099–1106.
23. Day, S. E.; Kettunen, M. I.; Gallagher, F. A.; De-En, H.; Lerche, M.; Wolber, J.; Golman, K.; Ardenkjaer-Larsen, J. H.; Brindle, K. M. *Detecting tumor response to treatment using hyperpolarized ^{13}C magnetic resonance imaging and spectroscopy. Nature Medicine* **2007***, 13(11)*, 1382–1387.
24. Golman, K.; Petersson, J. S.; Magnusson, P.; Johansson, E.; Åkeson, P.; Chai, C.; Hansson, G.; Månsson, S. *Cardiac metabolism measured noninvasively by hyperpolarized ^{13}C MRI. Magnetic Resonance in Medicine* **2008***, 59(5)*, 1005–1013.
25. Merritt, M. E.; Harrison, C.; Storey, C. J.; Sherry, A. D.; Malloy, C. R. *Inhibition of carbohydrate oxidation during the first minute of reperfusion after brief ischemia: NMR detection of hyperpolarized $^{13}CO_2$ and $H^{13}CO_{3-}$. Magnetic Resonance in Medicine* **2008***, 60(5)*, 1029-1036.

Parahydrogen-Induced Polarization

Pratip Bhattacharya, Ph.D.,
Huntington Medical Research Institute

Parahydrogen-Induced Polarization (PHIP) or Parahydrogen And Synthesis Allow Dramatically Enhanced Nuclear Alignment (PASADENA)[1] is a liquid state chemical technique of hyperpolarization which can be accomplished in seconds at room temperature. Dynamic Nuclear Polarization (DNP) is a solid state method of hyperpolarization where polarizations takes place at low temperature, high magnetic field, and with unpaired electron of selected species (e.g. triaryl radical) to produce strongly polarized nuclear spins in the solid state in hours. The solid sample is subsequently dissolved rapidly in water to create a solution of molecules with hyperpolarized nuclear spins.[2] DNP polarizer is now commercially available from Oxford Instruments. PHIP is usually accomplished in home-made polarizer systems.[3, 4] PHIP is limited to molecules with unsaturation (double or triple bonds) while DNP is a more general method and may be applied to a wider range of molecules. PHIP is a relatively inexpensive method of hyperpolarization compared to DNP and since the polarization can be accomplished in seconds to minutes in the PHIP polarizer, this technique can be used for several experimental trials within a short period of time. Both DNP and PHIP have been used for *in vivo* applications and real time metabolic and molecular imaging.

References

1. Bowers, C. R.; Weitekamp D. P.; Parahydrogen And Synthesis Allow Dramatically Enhanced Nuclear Alignment. *J. Am. Chem. Soc.* **1987***, 109*, 5541–5542.
2. Ardenkjaer-Larsen, J. H.; Fridlund, B.; Gram, A.; Hansson, G.; Hansson, L.; Lerche, M. H.; Servin, R.; Thaning, M.; Golman, K.; *Increase in signal-to-noise ratio of > 10,000 times in liquid-state NMR. Proceedings of the National Academy of Sciences of the United States of America* **2003***, 100(18)*, 10158–10163.
3. Hovener, J. B.; Chekmenev, E. Y.; Harris K., Perman, W. H.; Robertson, L., Ross, B. D.; Bhattacharya, P. PASADENA Hyperpolarization of ^{13}C Biomolecules: Equipment Design and Installation. *Magn Reson Mater Phy* **2009**, 22:111–121.
4. Hovener, J. B.; Chekmenev, E. Y.; Harris, K.; Perman, W. H.; Ross, B. D.; Bhattacharya, P. Quality Assurance of PASADENA Hyperpolarization for ^{13}C Biomolecules. *Magn Reson Mater Phy,* **2009**, 22:123–134.

Find the latest articles on DNP and PHIP hyperpolarization at **SigmaAldrich.com/mri**

MRI/MRS Products

The use of stable isotopes in MRI/MRS imaging has advanced exponentially, and we are committed to offering an extensive array of labeled compounds for your MRI/MRS research needs. We routinely offer an S&P tested grade for select products. We also have capabilities for manufacturing cGMP grade material upon request.

Researchers are using stable isotopes for advanced technologies such as hyperpolarization for *in vivo* MRI imaging[1,2] to create metabolic profiles to map and study alterations due to diseases. Dynamic Nuclear Polarization (**DNP**) and Para Hydrogen Induced Polarization (**PHIP**) are the two hyperpolarization techniques currently used in MRI. Each technique has its advantages that researchers are exploring for its potential in clinical applications.

Stable isotopes in conjunction with ^{13}C-MRS *in vivo* techniques provide a way to explore fluxes through energy related metabolic pathways. Various ^{13}C labeled glucose, pyruvate and lactate compounds elucidate tricarboxylic acid (TCA) cycle turnover and glutamate and glutamine metabolism.[3,4] As such, ^{13}C-MRS studies involves understanding metabolism at the molecular level.

Literature of Interest

1. Golman, K.; Zandt, R.; Thaning, M. M. *Proc Natl Acad Sci USA* **2006***, Jul 25: 103(30)*, 270–5. Real-time metabolic imaging.
2. Bhattacharya, P.; Chekmenev, E. Y.; Perman, W. H.; Harris, K. C.; Lin, A. P.; Norton, V. A.; Tan, C. T.; Ross, B. D.; Weitekamp, D. P. *J Magn Reson.* **2007,** *May: 186(1),* 50–5. Towards hyperpolarized ^{13}C-succinate imaging of brain cancer.
3. Nabuurs, C. L.; Klomp, D. W.; Veltien, A.; Kan, H. E.; Heerschap A. *Magn Reson Med*. **2008**, *Mar; 59(3)*,626–30. Localized sensitivity enhanced *in vivo* ^{13}C MRS to detect glucose metabolism in the mouse brain.
4. van der, Zijden, J. P.; van Eijsden, P.; de Graaf, R. A.; Dijkhuizen, R. M. *Brain* **2008**, *Aug; 131(Pt 8)*, 2209–19. 1H/13C MR spectroscopic imaging of regionally specific metabolic alterations after experimental stroke.

Compounds of Interest

Description	Isotopic Purity	Cat. No.
Acetic Acid-1-^{13}C	99 atom % ^{13}C	**279285**
Acetic Acid-2-^{13}C	99 atom % ^{13}C	**279307**
Acetic Acid-$^{13}C_2$	99 atom % ^{13}C	**282022**
Acetone-1,3-$^{13}C_2$	99 atom % ^{13}C	**299189**
Acetone-2-^{13}C	99 atom % ^{13}C	**299197**
Acetone-$^{13}C_3$	99 atom % ^{13}C	**491667**
Acetyl-1,2-$^{13}C_2$ Coenzyme A, lithium salt	99 atom % ^{13}C	**658650**
Acetylene Dicarboxylic Acid-1-^{13}C, disodium salt	99 atom % ^{13}C	**665223**
L-Alanine-1-^{13}C	99 atom % ^{13}C	**489867**
L-Alanine-2-^{13}C	99 atom % ^{13}C	**486779**
L-Alanine-3-^{13}C	99 atom % ^{13}C	**489948**
L-Alanine-2,3-$^{13}C_2$	99 atom % ^{13}C	**604682**
L-Alanine-$^{13}C_3$	99 atom % ^{13}C	**489875**
4-Amino-TEMPO-Piperidinyl-d_{17}	98 atom % D	**588741**
Ammonium-^{15}N Acetate	98 atom %^{15}N	**363006**
L-Asparagine-4-^{13}C monohydrate	99 atom % ^{13}C	**579866**
L-Aspartic Acid-1-^{13}C	99 atom % ^{13}C	**489972**
tert-Butan-2-^{13}C, d_9-ol	99 atom % ^{13}C, 98 atom % D	**679860**
Butyric Acid-1-^{13}C	99 atom % ^{13}C	**488372**
Butyric Acid-2-^{13}C	99 atom % ^{13}C	**588547**
Butyric-Acid-4,4,4-d_3	98 atom % D	**615706**
Choline-2-^{13}C,1,1,2,2-d_4 Chloride	99 atom % ^{13}C, 98 atom % D	**707996**
Choline-^{15}N Chloride	98 atom %^{15}N	**609269**
Diethyl Glutarate-$^{13}C_5$	99 atom % ^{13}C	**655708**
Ethanol-1-^{13}C	99 atom % ^{13}C	**324523**
Ethanol-2-^{13}C	99 atom % ^{13}C	**427047**
Ethanol-$^{13}C_2$	99 atom % ^{13}C	**427039**
Ethanol-$^{13}C_2$,d_5	99 atom % ^{13}C, 98 atom % D	**682586**
Ethanolamine-2-^{13}C	99 atom % ^{13}C	**606316**
Ethanolamine-$^{13}C_2$	99 atom % ^{13}C	**606294**
Ethanolamine-$^{13}C_2$·HCl	99 atom % ^{13}C	**606308**
Ethyl Acetoacetate-1,3-$^{13}C_2$	99 atom % ^{13}C	**485640**
Ethyl Acetoacetate-2,4-$^{13}C_2$	99 atom % ^{13}C	**485659**
Ethyl Acetoacetate-1,2,3,4-$^{13}C_4$	99 atom % ^{13}C	**489263**
Ethyl Pyruvate-3-^{13}C	99 atom % ^{13}C	**676594**
D-Fructose-1-^{13}C	99 atom % ^{13}C	**415553**
D-Fructose-$^{13}C_6$	99 atom % ^{13}C	**587621**
Fumaric Acid-2,3-$^{13}C_2$	99 atom % ^{13}C	**606073**
Fumaric Acid-$^{13}C_4$	99 atom % ^{13}C	**606014**
D-Galactose-1-^{13}C	99 atom % ^{13}C	**415545**
D-Galactose-1-^{13}C, S&P tested	99 atom % ^{13}C	**661406**
D-Galactose-2-^{13}C	99 atom % ^{13}C	**454621**
D-Galactose-$^{13}C_6$	99 atom % ^{13}C	**605379**
D-Glucose-1-^{13}C	99 atom % ^{13}C	**297046**
D-Glucose-1-^{13}C, S&P tested	99 atom % ^{13}C	**660655**
D-Glucose-2-^{13}C	99 atom % ^{13}C	**310794**
D-Glucose-2-^{13}C, S&P tested	99 atom % ^{13}C	**661457**
D-Glucose-6-^{13}C	99 atom % ^{13}C	**310808**
D-Glucose-6-^{13}C, S&P tested	99 atom % ^{13}C	**661430**
D-Glucose-1,2-$^{13}C_2$	99 atom % ^{13}C	**453188**
D-Glucose-1,2-, S&P tested	99 atom % ^{13}C	**661422**
D-Glucose-1,6-$^{13}C_2$	99 atom % ^{13}C	**453196**
D-Glucose-1,6-$^{13}C_2$, S&P tested	99 atom % ^{13}C	**661449**
D-Glucose-2,5-$^{13}C_2$	99 atom % ^{13}C	**605506**
D-Glucose-$^{13}C_6$	99 atom % ^{13}C	**389374**
D-Glucose-$^{13}C_6$, S&P tested	99 atom % ^{13}C	**660663**
D-Glucose-6,6-d_2	98 atom % D	**282650**
D-Glucose-6,6-d_2, S&P tested	98 atom % D	**661414**

Description	Isotopic Purity	Cat. No.
D-Glucose-C-d_7	98 atom % D	**552003**
L-Glutamic Acid-1-^{13}C	99 atom % ^{13}C	**604968**
L-Glutamic Acid-2-^{13}C	99 atom % ^{13}C	**605123**
L-Glutamic Acid-3-^{13}C	99 atom % ^{13}C	**490016**
L-Glutamic Acid-4-^{13}C	99 atom % ^{13}C	**587672**
L-Glutamic Acid-5-^{13}C	99 atom % ^{13}C	**492922**
L-Glutamic Acid-$^{13}C_5$	99 atom % ^{13}C	**604860**
L-Glutamic Acid-3,4-^{13}C	99 atom % ^{13}C	**691682**
L-Glutamine-1-^{13}C	99 atom % ^{13}C	**605018**
L-Glutamine-2-^{13}C	99 atom % ^{13}C	**605085**
L-Glutamine-3-^{13}C	99 atom % ^{13}C	**604941**
L-Glutamine-5-^{13}C (amide-^{13}C)	99 atom % ^{13}C	**604690**
L-Glutamine-1,2-$^{13}C_2$	99 atom % ^{13}C	**605220**
L-Glutamine-1,2-$^{13}C_2$, S&P tested	99 atom % ^{13}C	**660809**
L-Glutamine-$^{13}C_5$	99 atom % ^{13}C	**605166**
L-Glutamine-2-^{13}C,$^{15}N_1$ (amine-^{15}N)	99 atom % ^{13}C, 98 atom % ^{15}N	**608122**
Glycerol-2-^{13}C	99 atom % ^{13}C	**489484**
Glycerol-2-^{13}C, S&P tested	99 atom % ^{13}C	**661465**
Glycerol-1,3-$^{13}C_2$	99 atom % ^{13}C	**492639**
Glycerol-$^{13}C_3$	99 atom % ^{13}C	**489476**
Glycerol-$^{13}C_3$, S&P tested	99 atom % ^{13}C	**660701**
Glycerol-1,1,2,3,3-d_5	98 atom %D	**454524**
4-Hydroxy-TEMPO-d_{17}	98 atom %D	**487686**
4-Hydroxy-TEMPO-^{15}N	98 atom % ^{15}N	**705748**
L-Isoleucine-1-^{13}C	99 atom % ^{13}C	**604771**
Lauric Acid-1-^{13}C	99 atom % ^{13}C	**292168**
Lauric Acid-1-^{13}C, S&P tested	99 atom % ^{13}C	**660671**
L-Leucine-1-^{13}C	99 atom % ^{13}C	**490059**
L-Leucine-1,2-$^{13}C_2$, S&P tested	99 atom % ^{13}C	**604909**
L-Leucine-1-^{13}C,^{15}N	99 atom % ^{13}C, 98 atom % ^{15}N	**490067**
L-Leucine-2-^{13}C,^{15}N	99 atom % ^{13}C, 98 atom % ^{15}N	**607657**
L-Leucine-5,5,5-d_3	98 atom % D	**486825**
L-Leucine-5,5,5-d_3, S&P tested	98 atom % D	**661554**
L-Leucine-^{15}N	98 atom % ^{15}N	**340960**
Linoleic Acid-$^{13}C_{18}$	99 atom % ^{13}C	**605735**
L-Lysine-1-^{13}C·HCl, S&P tested	99 atom % ^{13}C	**660833**
D-Mannitol-1-^{13}C	99 atom % ^{13}C	**454613**
D-Mannitol-$^{13}C_6$	99 atom % ^{13}C	**605492**
D-Mannose-1-^{13}C	99 atom % ^{13}C	**415537**
Malonyl-$^{13}C_3$ Coenzyme A, lithium salt	99 atom % ^{13}C	**655759**
Myristic Acid-1-^{13}C	99 atom % ^{13}C	**490873**
Myristic Acid-1-^{13}C, S&P tested	99 atom % ^{13}C	**661155**
Myristic Acid-$^{13}C_{14}$	99 atom % ^{13}C	**605689**
Octanoic Acid-1-^{13}C	99 atom % ^{13}C	**296457**
Octanoic Acid-2-^{13}C	99 atom % ^{13}C	**591076**
Octanoic Acid-1,2,3,4-$^{13}C_4$	99 atom % ^{13}C	**493163**
Octanoyl-2,4,6,8-$^{13}C_4$ Coenzyme A, lithium salt	99 atom % ^{13}C	**703885**
Oleic Acid-1-^{13}C	99 atom % ^{13}C	**490423**
Oleic Acid-1-^{13}C, S&P tested	99 atom % ^{13}C	**661589**
Oleic Acid-1,2,3,7,8,9,10-$^{13}C_7$	99 atom % ^{13}C	**646458**
Oleic Acid-$^{13}C_{18}$	99 atom % ^{13}C	**490431**
Oleoyl-1-^{13}C-L-Carnitine·HCl	99 atom % ^{13}C	**597120**
Oleoyl-$^{13}C^{18}$-L-Carnitine·HCl	99 atom % ^{13}C	**644404**
Oleoyl-$^{13}C^{18}$ Coenzyme A, lithium salt	99 atom % ^{13}C	**675768**
4-Oxo-TEMPO-d_{16}	98 atom % D	**485268**
4-Oxo-TEMPO-1-^{15}N	98 atom % ^{15}N	**696471**

Description	Isotopic Purity	Cat. No.
4-Oxo-TEMPO-d_{16},^{15}N	98 atom % ^{15}N, 98 atom % D	**487740**
4-Oxo-TEMPO-d_{17},1-^{15}N	98 atom % ^{15}N, 98 atom % D	**591173**
Palmitic Acid-1-^{13}C	99 atom % ^{13}C	**292125**
Palmitic Acid-1-^{13}C, S&P tested	99 atom % ^{13}C	**661597**
Palmitic Acid-2-^{13}C	99 atom % ^{13}C	**492752**
Palmitic Acid-16-^{13}C	99 atom % ^{13}C	**605646**
Palmitic Acid-1,2-$^{13}C_2$	99 atom % ^{13}C	**485802**
Palmitic Acid-1,2,3,4-$^{13}C_4$	99 atom % ^{13}C	**489611**
Palmitic Acid-2,4,6,8, 10,12,14, 16-$^{13}C_8$	99 atom % ^{13}C	**605786**
Palmitic Acid-$^{13}C_{16}$	99 atom % ^{13}C	**605573**
Palmitic Acid-$^{13}C_{16}$, S&P tested	99 atom % ^{13}C	**679372**
Palmitoyl-1,2,3,4-$^{13}C_4$-L-Carnitine·HCl	99 atom % ^{13}C	**662127**
Palmitoyl-1-^{13}C Coenzyme A, lithium salt	99 atom % ^{13}C	**658200**
Palmitoyl-$^{13}C_{16}$ Coenzyme A, lithium salt	99 atom % ^{13}C	**655716**
L-Phenyl-1-^{13}C-alanine	99 atom % ^{13}C	**605042**
L-Phenylalanine-1-^{13}C	99 atom % ^{13}C	**490091**
L-Phenylalanine-2-^{13}C	99 atom % ^{13}C	**490113**
L-Phenylalanine-$^{13}C_9$, ^{15}N	99 atom % ^{13}C, 98 atom % ^{15}N	**608017**
Potassium Linoleate $^{13}C_{18}$	99 atom % ^{13}C	**605816**
Potassium Palmitate-1-^{13}C	99 atom % ^{13}C	**489646**
Potassium Palmitate-1-^{13}C, S&P tested	99 atom % ^{13}C	**661481**
Potassium Palmitate -1,2,3,4-$^{13}C_4$, S&P tested	99 atom % ^{13}C	**605808**
Potassium Palmitate -1,3,5,7,9-$^{13}C_5$	99 atom % ^{13}C	**676454**
Potassium Palmitate-$^{13}C_{16}$	99 atom % ^{13}C	**605751**
Propionic Acid-1-^{13}C	99 atom % ^{13}C	**282448**
L-Proline-1-^{13}C	99 atom % ^{13}C	**589497**
L-Proline-1-^{13}C, S&P tested	99 atom % ^{13}C	**661627**
Pyruvic-1-^{13}C Acid (free acid)	99 atom % ^{13}C	**677175**
Pyruvic-2-^{13}C Acid (free acid)	99 atom % ^{13}C	**692670**
L-Serine-1-^{13}C	99 atom % ^{13}C	**490156**
L-Serine-2-^{13}C,^{15}N	99 atom % ^{13}C, 98 atom % ^{15}N	**485985**
Sodium Acetate-1-^{13}C	99 atom % ^{13}C	**279293**
Sodium Acetate-1-^{13}C, S&P tested	99 atom % ^{13}C	**668656**
Sodium Acetate-2-^{13}C	99 atom % ^{13}C	**279315**
Sodium Acetate-2-^{13}C, S&P tested	99 atom % ^{13}C	**660310**
Sodium Acetate-$^{13}C_2$	99 atom % ^{13}C	**282014**
Sodium Acetate-$^{13}C_2$, S&P tested	99 atom % ^{13}C	**663859**
Sodium Butyrate-1-^{13}C	99 atom % ^{13}C	**292656**
Sodium Butyrate-2-^{13}C	99 atom % ^{13}C	**485357**
Sodium Butyrate-3-^{13}C	99 atom % ^{13}C	**588563**

Description	Isotopic Purity	Cat. No.
Sodium Butyrate-1,2-$^{13}C_2$	99 atom % ^{13}C	**603929**
Sodium Butyrate-2,4-$^{13}C_2$	99 atom % ^{13}C	**492000**
Sodium Butyrate-$^{13}C_4$	99 atom % ^{13}C	**488380**
Sodium Dichloroacetate-$^{13}C_2$	99 atom % ^{13}C	**707198**
Sodium D-3-Hydroxybutyrate-1,2-$^{13}C_2$, S&P tested	99 atom % ^{13}C	**660302**
Sodium D-3-Hydroxybutyrate-1,3-$^{13}C_2$	99 atom % ^{13}C	**606111**
Sodium D-3-Hydroxybutyrate-2,4-$^{13}C_2$	99 atom % ^{13}C	**674117**
Sodium DL-3-Hydroxybutyrate-1-^{13}C	99 atom % ^{13}C	**696323**
Sodium DL-3-Hydroxybutyrate-4-^{13}C	99 atom % ^{13}C	**492302**
Sodium DL-3-Hydroxybutyrate-1,3-$^{13}C_2$	99 atom % ^{13}C	**488895**
Sodium DL-3-Hydroxybutyrate-2,4-$^{13}C_2$	99 atom % ^{13}C	**492299**
Sodium DL-3-Hydroxybutyrate-$^{13}C_4$	99 atom % ^{13}C	**606030**
Sodium D-Lactate-3-^{13}C solution	99 atom % ^{13}C	**676144**
Sodium L-Lactate-1-^{13}C solution	99 atom % ^{13}C	**606022**
Sodium L-Lactate-2-^{13}C solution	99 atom % ^{13}C	**589209**
Sodium L-Lactate-3-^{13}C solution	99 atom % ^{13}C	**490040**
Sodium L-Lactate-2,3-$^{13}C_2$ solution	99 atom % ^{13}C	**606006**
Sodium L-Lactate-$^{13}C_3$ solution	99 atom % ^{13}C	**485926**
Sodium L-Lactate-2-d_1 solution	99 atom % ^{13}C	**589217**
Sodium Octanoate-2,4,6,8-$^{13}C_4$	99 atom % ^{13}C	**657204**
Sodium Propionate-1-^{13}C	99 atom % ^{13}C	**279455**
Sodium Propionate-2-^{13}C	99 atom % ^{13}C	**490660**
Sodium Propionate-3-^{13}C	99 atom % ^{13}C	**490679**
Sodium Propionate –1,2-$^{13}C_2$	99 atom % ^{13}C	**493325**
Sodium Propionate-2,3-$^{13}C_2$	99 atom % ^{13}C	**493333**
Sodium Propionate-$^{13}C_3$	99 atom % ^{13}C	**490636**
Sodium Propionate-$^{13}C_3$, S&P tested	99 atom % ^{13}C	**660949**
Sodium Pyruvate-1-^{13}C	99 atom % ^{13}C	**490709**
Sodium Pyruvate-2-^{13}C	99 atom % ^{13}C	**490725**
Sodium Pyruvate-3-^{13}C	99 atom % ^{13}C	**490733**
Sodium Pyruvate-1,2-$^{13}C_2$	99 atom % ^{13}C	**493392**
Sodium Pyruvate-2,3-$^{13}C_2$	99 atom % ^{13}C	**486191**
Sodium Pyruvate-$^{13}C_3$	99 atom % ^{13}C	**490717**
Sodium Pyruvate-$^{13}C_3$, S&P tested	99 atom % ^{13}C,	**660957**
Sodium Pyruvate-2-^{13}C, 3,3,3-d_3	99 atom % ^{13}C, 97 atom % D	**702242**
Stearic Acid-1-^{13}C	99 atom % ^{13}C	**299162**
Stearic Acid-2-^{13}C	99 atom % ^{13}C	**591491**
Stearic Acid-$^{13}C_{18}$	99 atom % ^{13}C	**605581**
Stearoyl-$^{13}C_{18}$ Coenzyme A, lithium salt	99 atom % ^{13}C	**675776**
Succinic Acid-1,4-$^{13}C_2$	99 atom % ^{13}C	**485349**
Sucrose-$^{13}C_{12}$	99 atom % ^{13}C	**605417**
D-Xylose-1-^{13}C	99 atom % ^{13}C	**331104**
D-Xylose-$^{13}C_5$	98 atom % ^{13}C	**666378**

Sterility and Pyrogen Tested Material

To prepare these products, our research grade material receives extra processing and testing. Our bulk material receives extra filtering and special handling to control the microbial content of the product. The bulk material is tested for Bacterial Endotoxins and Sterility. The testing is done in bulk form, before subdivision packaging. This bulk test does not guarantee that the subdivision or repackaged aliquot is sterile and pyrogen free when it is received or used by the customer, and does not imply suitability for any particular purpose. If the product must be sterile and pyrogen free for the intended application, we recommend that the product be tested prior to actual use.

Isotopically Labeled Oxygen and Water

Use of ^{17}O or deuterated labeled water in imaging allows researchers to obtain better contrast images and aid in understanding effects of different physiological conditions in an abnormal state. Water-^{17}O and Oxygen-^{17}O have been used in MRI to measure cerebral blood flow and to study oxidative metabolism for neurological disorders.[1–3] Deuterium oxide (D_2O), a non-visible signal in proton MR has been effectively used with *in vivo* MRI-based techniques to obtain measurement of water fluxes or contrast images.[4]

Labeled Oxygen and Water

Description	Isotopic Purity	Cat. No.
Oxygen-$^{17}O_2$ (gas)	70 atom % ^{17}O	**602779**
Oxygen-$^{17}O_2$ (gas)	60 atom % ^{17}O	**602809**
Oxygen-$^{17}O_2$ (gas)	45 atom % ^{17}O	**602817**
Water-^{17}O	90 atom % ^{17}O	**609862**
Water-^{17}O	80–84.9 atom % ^{17}O	**618535**
Water-^{17}O	75–80.9 atom % ^{17}O	**603066**
Water-^{17}O	40–44.9 atom % ^{17}O	**602965**

Description	Isotopic Purity	Cat. No.
Water-^{17}O	35–39.9 atom % ^{17}O	**603007**
Water-^{17}O	25–29.9 atom % ^{17}O	**603023**
Water-^{17}O	7–9.9 atom % ^{17}O	**645907**
Deuterium Oxide	99.9 atom % D	**151882**
Deuterium Oxide	99.8 atom % D	**617385**
Deuterium Oxide	99 atom % D	**435767**
Deuterium Oxide	70 atom % D	**613428**

Literature of Interest

1. Zhu, X. H.; Zhang, N.; Zhang, Y.; Zhang, X.; Ugurbil, K.; Chen W. *NMR Biomed*. **2005**, *Apr;18(2)*, 83–103 In vivo ^{17}O NMR approaches for brain study.
2. Tailor, D. R.; Baumgardner, J. E.; Regatte, R. R.; Leigh, J. S.; Reddy, R. *Neuroimage* **2004**, *Jun;22(2)*, 611–8 Proton MRI of metabolically produced $H_2{}^{17}O$ using an efficient $^{17}O_2$ delivery system.
3. Zhang, N.; Zhu, X. H.; Lei, H.; Ugurbil, K.; Chen, W. J. Cereb *Blood Flow Metab.* **2004**, *Aug;24(8)*, 840–8 Simplified methods for calculating cerebral metabolic rate of oxygen based on ^{17}O magnetic resonance spectroscopic imaging measurement during a short $^{17}O_2$ inhalation.
4. Leung, V. Y. L., et al. O*steoarthritis and Cartilage,* **2008**, *Nov. 16(11),* 1312–1318. Age-related degeneration of lumbar intervertebral discs in rabbits revealed by deuterium oxide-assisted MRI.

Nitroxyl Radicals

Nitroxyl radicals are the source for the unpaired electrons needed during the hyperpolarization of a substrate. Labeled radicals can improve the polarization process. Our Stable Isotopes group is committed to design and offer these radicals to enhance your research.

Description	Isotopic Purity	Cat. No.
4-Amino-TEMPO-piperidinyl-d_{17}	98 atom % D	**588741**
4-Hydroxy-TEMPO-d_{17}	98 atom % D	**487686**
4-Hydroxy-TEMPO-^{15}N	98 atom % ^{15}N	**705748**
4-Oxo-TEMPO-d_{16}	97 atom % D	**485268**
4-Oxo-TEMPO-1-^{15}N	98 atom % ^{15}N	**696471**
4-Oxo-TEMPO-d_{16},^{15}N	98 atom % ^{15}N	**487740**
4-Oxo-TEMPO-d_{17},1-^{15}N	98 atom % ^{15}N	**591173**

Did you know
more than 3,000 people conduct research in Antarctica each year?

And that Sigma-Aldrich, provider of ISOTEC® Stable Isotopes, has over 3,000 labeled products for your research needs.

Hyperpolarization Using Noble Gases

The challenges of using radioactive gases and obtaining high contrast images of lung for various ventilation disorders, are now answered by images taken after inhalation of hyperpolarized noble gases. ^{3}Helium (^{3}He) or ^{129}Xenon (^{129}Xe) can be hyperpolarized by optical pumping of the Rubidium atom via a spin-exchange collision mechanism to obtain higher contrast images for diagnostic lung imaging.[1,2] There are also studies conducted to obtain "real-time" images by simultaneously using hyperpolarized ^{13}C substrates with ^{3}He.[3] The use of ^{129}Xe also offers the potential for imaging organs other than lungs for circulatory disorders, due to its diffusion properties in blood and tissues.

Hyperpolarization of noble gases such as ^{3}He and ^{129}Xe offers the following benefits in imaging:

- Provides high contrast images for diagnostic testing in lung imaging
- Allows rapid dynamic imaging using ^{3}He for various ventilation defects
- Increases the sensitivity of these gases by a factor of 100,000[4]
- ^{129}Xe has the potential to image other organs due to its diffusion properties after inhalation

Noble Gases

Description	Isotopic Purity	Cat. No.
Helium-^{3}He (Isotopic Grade)	99.9999 atom %	**600253***
Helium-^{3}He (Chem Pure Grade)	99.95 atom %	**600245***
Xenon-^{129}Xe	99.95 atom % ^{129}Xe	**593923**
Xenon-^{129}Xe	80 atom % ^{129}Xe	**602140**
Xenon-^{129}Xe	70 atom % ^{129}Xe	**602132**

*Due to market fluctuations, please inquire about Helium-^{3}He availability

Literature of Interest

1. Fain, S. B.; Korosec, F. R.; Holmes, J. H.; O'Halloran, R.; Sorkness, R. L.; Grist, T.; *M. J Magn Reson Imaging.* **2007**, *May; 25(5),* 910–23. Review. Functional lung imaging using hyperpolarized gas MRI.
2. Mugler, J.P. 3rd; Wang, C.; Miller, G. W.; Cates, G. D. Jr.; Mata, J. F.; Brookeman, J. R.; de Lange, E. E.; Altes, T. A. *Acad. Radiol* **2008**, *Jun; 15(6)*, 693–701. Helium-3 diffusion MR imaging of the human lung over multiple time scales.
3. Golman, K.; Olsson, L. E.; Axelsson, O.; Månsson, S.; Karlsson, M.; Petersson, J. S. *Br J Radiol* **2003**, *76 Spec No 2:S*, 118–27. Molecular imaging using hyperpolarized ^{13}C.
4. Möller, H. E.; Chen, J. X.; Saam, B.; Hagspiel, K. D.; Johnson, G. A.; Altes, T. A.; de Lange, E. E. *Hans-Ulrich Kauczor Magnetic Resonance in Medicine* **2002**, *Jun;47(6)*, 1029–51. MRI of the lungs using hyperpolarized noble gases.

Visit us on the Web

- Link to pages dedicated to specific product applications such as MRI/MRS and Metabolic Research
- View technology web spotlights and the latest products
- Access our extensive product catalog
- Download product literature including flyers, brochures and technical articles
- Request a quotation for stable isotope products or custom synthesis projects

Toolbox

- Molecular weight calculator for labeled compounds
- Substructure search
- Links to related sections of the Sigma-Aldrich® Website such as Labware and the Solvent Center

These are just a few highlights of the information available on our Website.

To learn more, please visit us at **SigmaAldrich.com/isotec**

Stable Isotopes in PET

Labeled isotopes used as target materials in imaging have provided insights into understanding various mechanisms of the human physiology and for treatment of diseases. In the PET industry, Water-^{18}O is widely used for the production of ^{18}F radionuclides such as ^{18}FDG (Fluoro-deoxyglucose). ^{18}FDG has been used for PET in conjunction with other imaging modalities (CT/SPECT) to diagnose and treat a wide range of diseases from malignancies in the lungs, liver and brain tumors to other neurological disorders such as epilepsy and Alzheimer's.[1–3] Water-^{16}O is a target material for producing ^{13}N radionuclides such as ^{13}N-Ammonia used for PET myocardial perfusion imaging.[4,5]

Literature of Interest

1. Hoh, C. K. *Nucl Med Biol*. **2007**, *Oct;34(7)*, 737–42. Clinical use of FDG PET.
2. Morooka, M.; Kubota, K.; Murata, Y.; Shibuya, H.; Ito, K.; Mochizuki, M.; Akashi, T.; Chiba, T.; Nomura, T.; Ito, H.; Morita, Ann, T. *Nucl Med.* **2008**, *Aug;22(7)*, 635–9. (1 8)F-FDG-PET/CT findings of granulocyte colony stimulating factor (G-CSF)-producing lung tumors.
3. Fischman, A. J. *Cancer Treat Res*. **2008**, *143*, 67–92. PET Imaging of Brain Tumors.
4. Alexánderson, E.; Gómez-León, A.; Vargas, A.; Romero, J. L.; Sierra Fernández, C.; Rodriguez, Valero M.; García-Rojas, L.; Meave, A.; Amigo, M. C. *Rheumatology (Oxford).* **2008**, *Jun; 47 (6)*, 894–6. Myocardial ischaemia in patients with primary APS: a ^{13}N-ammonia PET assessment.
5. Mullani, N. A.; Herbst, R. S.; O'Neil, R. G.; Gould, K. L.; Barron, B. J.; Abbruzzese, J. L. J *Nucl Med*. **2008**, *Apr;49(4)*, 517–23. Tumor blood flow measured by PET dynamic imaging of first-pass ^{18}F-FDG uptake: a comparison with ^{15}O-labeled water-measured blood flow.

Labeled Target Material

Description	Isotopic Purity	Cat. No.
Water-^{18}O	97 atom % ^{18}O	**329878**
$^{15}N_2/O_2$(RG) Gas Mix Ratio 39:1	99 atom % ^{15}N	**600911**
$^{15}N_2/O_2$(RG) Gas Mix Ratio 39:1	95 atom % ^{15}N	**601020**
Oxygen-$^{18}O_2$ (gas)	99 atom % ^{18}O	**602892**

Additional Products for PET Imaging

Description	Isotopic Purity	Cat. No.
2-Chloro-2-deoxy-D-glucose		**C203**
2-Deoxy-2-fluoro-D-glucose		**F5006**
4,7,13,16,21,24-Hexaoxa-1, 10-diazabicyclo[8.8.8] hexacosane		**291110**
Mannose Triflate		**M1568**
Nitrogen-^{14}N (gas)	99.99 atom % ^{14}N	**608661**
Water-^{16}O	99.99 atom % ^{16}O	**329886**

Water-^{18}O, 97 atom % for PET Imaging

PET specialists expect consistent, high-quality Water-^{18}O and our Quality Control department verifies that all of our Water-^{18}O meet these requirements. QC test results for each batch are displayed on the Certificate of Analysis, accessible at **SigmaAldrich.com**

Test	Methods	Specification
Appearance	Visual	Clear, colorless, free of visible particulate matter
Isotopic Composition (Normalized with respect to Hydrogen isotopes)	MS	Minimum 97 atom% ^{18}O Report ^{17}O atom% Report ^{16}O atom%
Conductivity		≤ 5 µS/cm or µmho/cm
pH		5.5–8.0
Organic Carbon	TOC	≤ 5 ppm
Copper	ICP	≤ 1 ppm
Total Iron/Iron	ICP	≤ 1 ppm
Zinc	ICP	≤ 2 ppm
Calcium	IC	≤ 1 ppm
Potassium	IC	≤ 1 ppm
Magnesium	IC	≤ 1 ppm
Sodium	IC	≤ 2 ppm
Phosphorus/Phosphate	IC	≤ 1 ppm
Sulfur/Sulfate	IC	≤ 1 ppm
Bromide	IC	≤ 1 ppm
Chloride	IC	≤ 1 ppm
Fluoride	IC	≤ 1 ppm
Nitrate	IC	≤ 1 ppm
Ammonium	IC	≤ 1 ppm
Bioburden		≤ 100 CFU/mL
Pyrogen	LAL	≤ 0.25 EU/mL

Catalog No.:
329878

Linear Formula:
$H_2{}^{18}O$

Molecular Weight:
20.02

CAS No.:
14314-42-2

Packaging Specifications:

- Type 1 serum glass vial (or borosilicate)
- Gray butyl rubber, Teflon-coated stopper
- Aluminum crimp seal
- Packaging: 1 g, 0.25 g units

To request our bulk quote email
isosales@sial.com

Let Us Help You Design Your Stable Isotope-Labeled Molecule

Our Custom Synthesis Expertise Enhances your Research

Cutting-edge research in MRI, MRS and especially hyperpolarization imaging, demands unique molecules with selective stable isotope labeling patterns. Our custom synthesis team is ready to work with you to design your molecule. We are ready to understand your research needs and, working together, we can come up with the best strategies to help you achieve your goals. We will do our best to work within your budget and provide a cost-effective solution. We also have access to a reliable, consistent supply of raw materials from Sigma-Aldrich®, including our extensive inventory of stable isotope-labeled compounds.

Our knowledge, experience and resources, combined with our on-site production capabilities, enable us to perform multi-step, complex syntheses to meet your requirements. All of these advantages allow us to shorten the delivery time and provide you with the highest quality product for your research. Our sales team will actively communicate the status of your project to you. We are ready to support your research project.

To discuss your project or request a custom synthesis quotation, please contact the ISOTEC® Stable Isotope Technical Service Group at **isosales@sial.com**.

C. T. Tan, Ph.D., Stable Isotopes Lead

For more information on these services or to request a custom quote, contact:

Stable Isotopes Customer Service
Phone: (937) 859-1808
U.S. and Canada: (800) 448-9760
Fax: (937) 859-4878
Email: **isosales@sial.com**
Website: **SigmaAldrich.com/isotec**

MilliporeSigma
400 Summit Drive
Burlington, MA 01803

PB8642ENUS, KXW
2017 - 05898
11/2017